

Electronic Supplementary Material (ESI) for Journal of Materials Chemistry C

This journal is © The Royal Society of Chemistry 2023

Transform Quinoline Derivatives from ACQ to AIE: Modulating Substituent Electronic Effects to Alter Excited State Reorganization Energy Distribution

Longjie Wang,^{‡a} Yuchen Zhang,^{‡b} Xiangdi Huang,^a Yanxiong Liu,^a Yi Cheng,^a Wenwen Fan,^a Liyan Zheng,^{*a} and Qiue Cao^{*a}

a. School of Chemical Science and Technology, Key Laboratory of Medicinal Chemistry for Natural Resource, Yunnan University, No. 2 North Cuihu Road

b. Key Laboratory of Organofluorine Chemistry, Shanghai Institute of Organic Chemistry, Chinese Academy of Sciences, 345 Lingling Road, Shanghai 200032, China

[‡] These authors contributed equally to this work.

E-mail: zhengliyan@ynu.edu.cn ; qecao@ynu.edu.cn

Materials

All chemicals and reagents are purchased from Aladdin Company. The final products used in all experiments were purified on the silica gel column and recrystallized at least twice.

Measurement

^1H , ^{13}C -NMR spectra were recorded on AVANCE DRX 400 spectrometer (Bruker, German). HPLC-MS were measured by electrospray ionization mass spectra with a High Performance 1100 Liquid Chromatography-Mass Spectrometer (Agilent Technologies, USA). A C18 column (250 mm* 4.6 mm, 5 μm , Hypersil GOLD, USA) was deployed as stationary phase. Digital photos were taken with the iPhone XR smartphone. Single-crystal X-ray diffraction (XRD) data were collected on a Rigaku Oxford Diffraction Supernova with Atlas Diffractometer, and crystal structures were solved with Olex2. Fluorescence spectra in the range of 300-700 nm were recorded with the F-4700 fluorescence spectrophotometer (HITACHI, Japan) at room temperature. Fluorescence decay curves measured by 285 nm and 390 nm excitation from Nano LED lamp were obtained on Horiba Jobin Yvon Fluorolog-3 spectrofluorometer. Fluorescence spectra, phosphorescence spectra and fluorescence quantum yields were measured on Horiba Jobin Yvon Fluorolog-3 spectrofluorometer. The size of nanoparticles in the solution was determined by NanoBrook Omni (Bruker, USA).

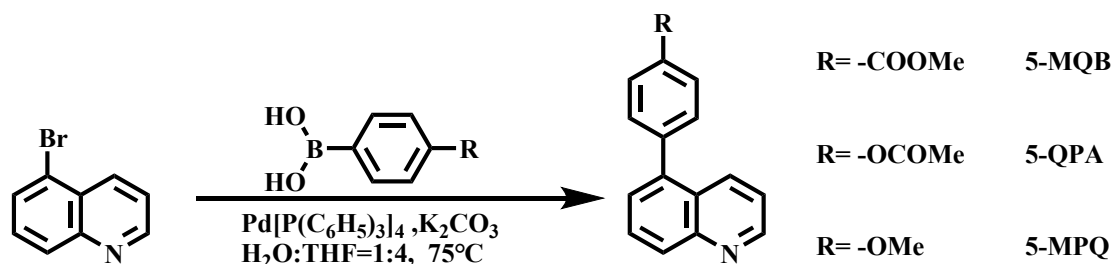
Computational Details

All the compounds were fully optimized with the density functional theory (DFT) in gaussian 09 method by using PBE0 density functional and def2svp basis set.¹ The SMD implicit solvation model was used to simulate the effect of solvent molecules on molecular properties through dielectric constant refraction. The reorganization energy was analyzed by Dushin software². The excited state structures of these compounds in crystal environment were simulated by quantum mechanics and molecular mechanics methods (QM/MM) which contained the QM part at PBE0/def2svp level and the MM part with the universal forcefield (UFF) in the Gaussian 09 package. The natural transition orbits of excited electrons were analyzed by Multiwfn and VMD programs.³

Culture and analysis of single crystals

The single crystals of 5-MQB, 5-QPA and 5-MPQ were grown via evaporation of a mixed solvent of ethyl acetate and n-hexane, while the single crystal of 5-QBA was obtained from a solution of dimethylacetamide and diethyl ether. The corresponding Cambridge Crystallographic Data Centre (CCDC) numbers for these crystals are 2255887, 2255889, 2255886, and 2255887, respectively. The Hirshfeld surfaces and decomposed fingerprint plots were calculated and mapped using CrystalExplorer 17.5 package.⁴ Single crystal analysis was conducted by olex2 software.⁵

Compounds Synthesis Method



methyl 4-(quinolin-5-yl)benzoate (5-MQB)

5-bromoquinoline (5.00 mmol, 1.0300 g) and (4-(methoxycarbonyl)phenyl)boronic acid (7.00 mmol, 1.2600 g) were added into a 100.0 mL two-necked flask with 20.0 ml THF, potassium carbonate (0.5000 g, 3.62 mmol) were dissolved in 5.0 mL water and these two solutions were mixed; then, (0.10 mmol, 0.1156 g) (beta-4)-platinum were added into this mixture. After stirring at 75 °C for 48 h under nitrogen gas, the reaction mixture was diluted with water and extracted with ethyl acetate. The organic layer was separated, washed with water and brine, dried with enough anhydrous sodium sulphate. After filtration, the filtrate was evaporated under reduced pressure and the crude product was purified on a silica gel column using petroleum/ether ethyl acetate (10/1, v/v) as eluent. 1.1243 g colorless powder of 5-MQB was obtained with 85.5% yield. ¹H NMR (400 MHz, Chloroform-*d*) δ 8.95 (dd, *J* = 4.2, 1.7 Hz, 1H), 8.18 (dd, *J* = 7.8, 5.9 Hz, 4H), 7.78 (dd, *J* = 8.6, 7.0 Hz, 1H), 7.61 – 7.49 (m, 3H), 7.38 (dd, *J* = 8.6, 4.2 Hz, 1H), 3.98 (s, 3H). ¹³C NMR (400 MHz, Chloroform-*d*) δ 168.2, 154.0, 148.5, 144.1, 139.3, 134.9, 130.1, 129.8, 129.6, 129.5, 128.9, 127.3, 126.4, 121.3. HRMS: *m/z*: calculated for C₁₇H₁₃NO₂: 263.0946; found: 264.1034 [M+H]⁺.

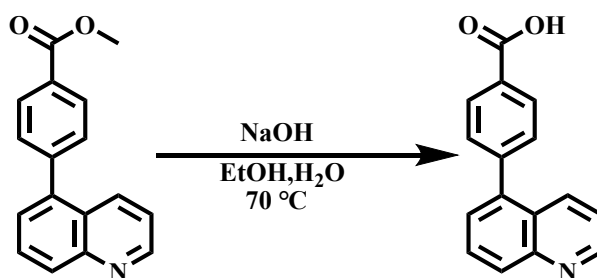
4-(quinolin-5-yl)phenyl acetate (5-QPA)

5-bromoquinoline (5.00 mmol, 1.0300 g) and (4-acetoxyphenyl)boronic acid (7.00 mmol, 1.2600 g) were added into a 100.0 mL two-necked flask with 20.0 ml THF, potassium carbonate (0.5000 g, 3.62 mmol) were dissolved in 5.0 mL water and these two solutions were mixed; then, (0.10 mmol, 0.1156 g) (beta-4)-platinum were added. After stirring at 75 °C for 48 h under nitrogen gas, the reaction mixture was diluted with water and extracted with ethyl acetate. The organic layer was separated, washed with water and brine, dried with enough anhydrous sodium sulphate. After filtration, the filtrate was evaporated under reduced pressure and the crude product was purified on a silica gel column using petroleum/ether ethyl acetate (3/1, v/v) as eluent. 1.0678 g colorless powder of 5-QPA was obtained with 81.2% yield. ¹H NMR (400 MHz, Chloroform-*d*) δ 8.93 (d, *J* = 4.7 Hz, 1H), 8.24 (d, *J* = 8.5 Hz, 1H), 8.14 (d, *J* = 8.4 Hz, 1H), 7.75 (t, *J* = 7.8 Hz, 1H), 7.49 (s, 1H), 7.47 (d, *J* = 7.9 Hz, 2H), 7.36 (dd, *J* = 8.7, 4.0 Hz, 1H), 7.24 (d, *J* = 7.2 Hz, 2H), 2.36 (s, 3H). ¹³C NMR (400 MHz, Chloroform-*d*) δ 170.2, 152.3, 148.4, 140.7, 136.5, 134.3, 131.7, 129.1, 129., 127.4, 127.4, 126.6, 121.70, 121.1, 21.2. HRMS: *m/z*: calculated for C₁₇H₁₃NO₂: 263.0946; found: 264.1019 [M+H]⁺.

5-(4-methoxyphenyl)quinoline (5-MPQ)

5-bromoquinoline (5.00 mmol, 1.0300 g) and (4-ethylphenyl)boronic acid (7.00 mmol, 1.0500 g) were added into a 100.0 mL two-necked flask with 20.0 ml THF, potassium carbonate (0.5000 g, 3.62 mmol) were dissolved in 5.0 mL water and these two solutions were mixed; then, (0.10 mmol, 0.1156 g) (beta-4)-platinum were added. After stirring at 75 °C for 48 h under nitrogen gas, the reaction mixture was diluted with water and extracted with ethyl acetate. The organic layer was separated, washed with water and brine, dried with enough anhydrous sodium sulphate. After filtration, the filtrate was evaporated under reduced pressure and the crude product was purified on a silica gel column using petroleum/ether ethyl acetate (10/1, v/v) as eluent. 1.0579 g colorless powder of QLP-5 was obtained with 90.0% yield. ¹H NMR (400 MHz, Chloroform-*d*) δ(ppm): 8.92 (dd, *J* = 4.2, 1.8 Hz, 1H), 8.28 – 8.26 (m, 1H), 8.12 – 8.10 (m, 1H), 7.74 (dd, *J* = 8.6, 7.1 Hz, 1H), 7.50 – 7.48 (m, 1H), 7.40 – 7.38 (m, 2H), 7.37 – 7.34 (m, 1H), 7.06 – 7.03 (m, 2H), 3.89 (s, 3H). ¹³C NMR (400 MHz, Chloroform-*d*) δ(ppm): 159.2, 150.1, 148.5, 140.1, 134.5, 131.6, 131.1, 128.9, 128.5, 127.2, 126.9, 120.9, 113.9, 55.3. HRMS: *m/z*: calculated for C₁₆H₁₃NO: 235.0997; found: 236.1069 [M+H]⁺.

4-(quinolin-5-yl)benzoic acid (5-QBA)



methyl 4-(quinolin-5-yl)benzoate (5mmol, 1.3100 g) were added into a 500.0 mL two-necked flask with 80.0 ml EtOH, NaOH(10 mmol, 0.4000 g) were dissolved in 20.0 mL water and these two solutions were mixed. After stirring at 70 °C for 12 h, the reaction mixture was diluted with water and adjust the pH to 4.0 with 1M HCl aqueous solution, then extracted with ethyl acetate. The organic layer was separated, washed with water and brine, dried with enough anhydrous sodium sulphate. After filtration, the filtrate was evaporated under reduced pressure and recrystallized with ethanol and water, obtaining 0.7450g colorless powder of 5-QBA with 60.0% yield. ¹H NMR (400 MHz, DMSO-*d*₆) δ 12.95 (s, 1H), 8.93 (dd, *J* = 4.1, 1.8 Hz, 1H), 8.47 (dd, *J* = 8.3, 1.8 Hz, 1H), 8.07 (d, *J* = 2.6 Hz, 1H), 8.05 (d, *J* = 4.3 Hz, 2H), 7.83 (dd, *J* = 7.2, 1.5 Hz, 1H), 7.79 (d, *J* = 8.3 Hz, 2H), 7.75 – 7.70 (m, 1H), 7.60 (dd, *J* = 8.3, 4.1 Hz, 1H). ¹³C NMR (400 MHz, DMSO-*d*₆) δ 169.1, 150.9, 145.4, 144.1, 140.0, 137.9, 131.2, 130.7, 129.8, 129.1, 129.0, 128.8, 126.9, 122.0. HRMS: *m/z*: calculated for C₁₆H₁₁NO₂: 249.0790; found: 248.0716 [M-H]⁻.

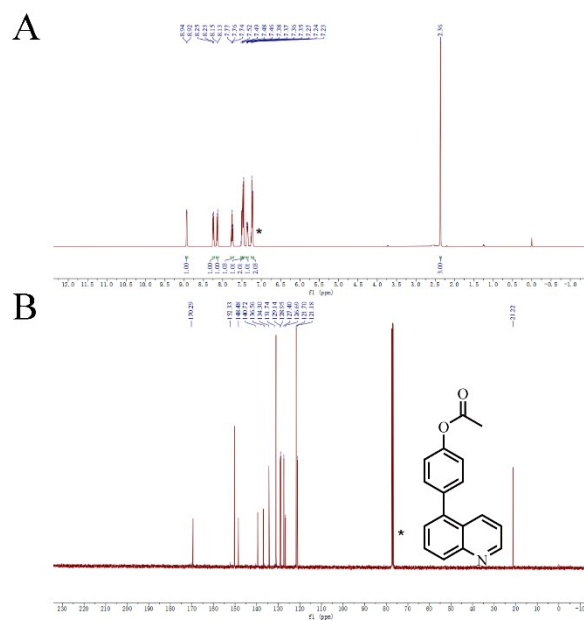


Figure S3. (A) ^1H and (B) ^{13}C NMR spectra of 5-QPA. The solvent peaks were marked as asterisk.

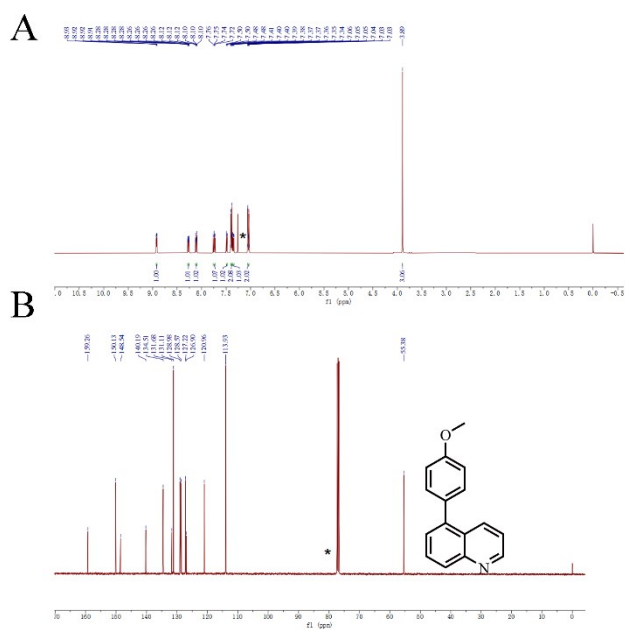


Figure S4. (A) ^1H and (B) ^{13}C NMR spectra of 5-MPQ. The solvent peaks were marked as asterisk.

High Resolution Mass Spectrometry

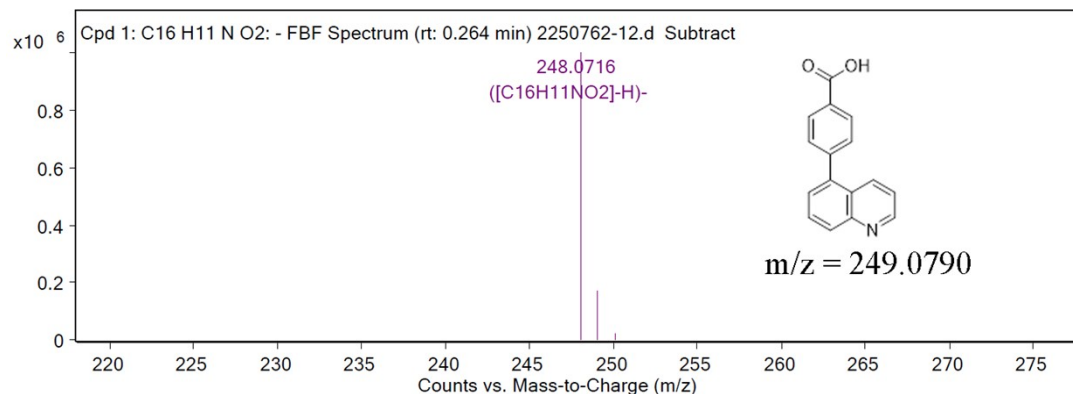


Figure S5. High resolution mass spectrum of 5-QBA with chemical ionization.

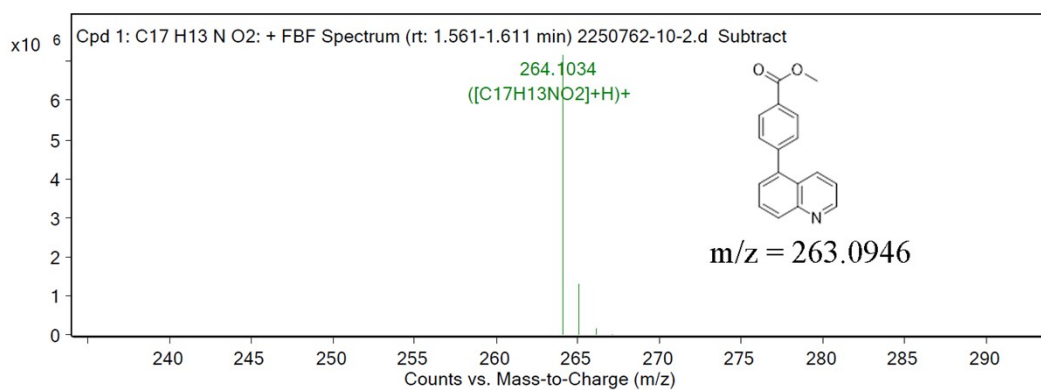


Figure S6. High resolution mass spectrum of 5-MQB with chemical ionization.

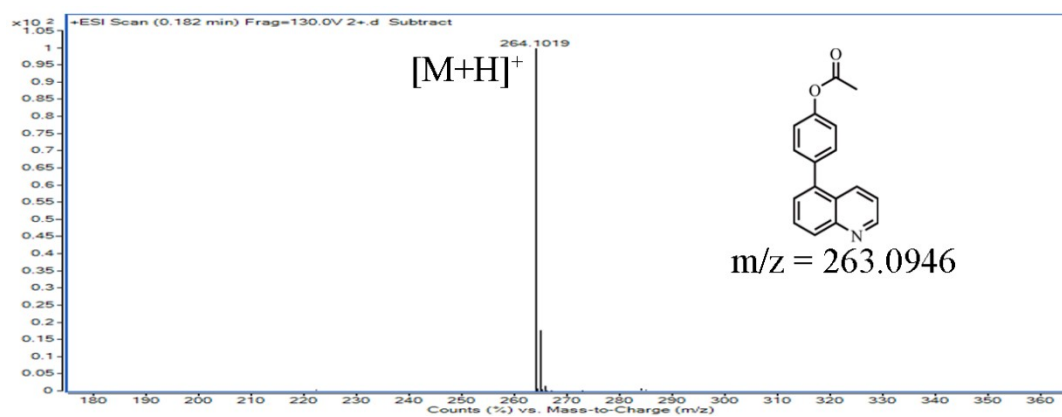


Figure S7. High resolution mass spectrum of 5-QPA with chemical ionization.

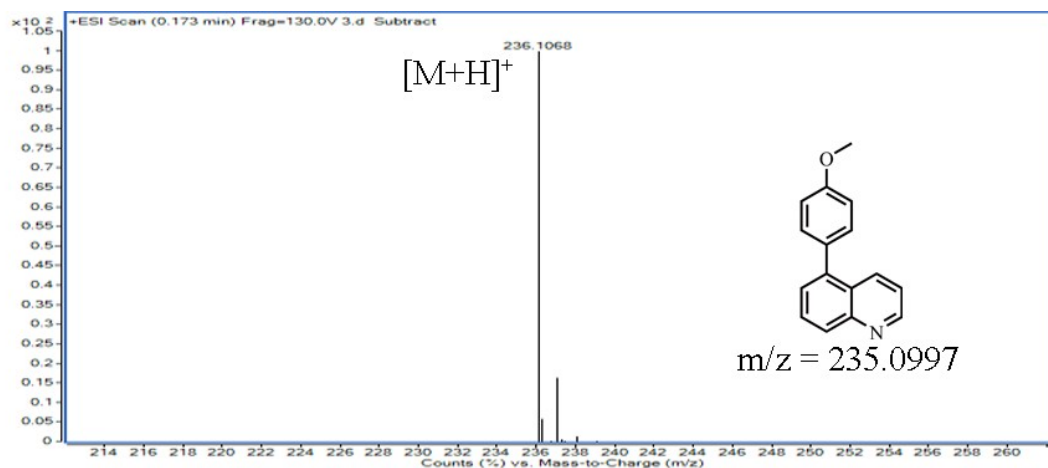


Figure S8. High resolution mass spectrum of 5-MPQ with chemical ionization.

Size Distribution

Table S1. The size distribution of 5-QBA in the different solvent systems. Concentration = 10^{-5} M.

	particle size (nm)	Polydispersity
$V_{H_2O} : V_{DMA} = 7:3$	116.3	0.031
$V_{H_2O} : V_{DMA} = 8:2$	212.5	0.047
$V_{H_2O} : V_{DMA} = 9:1$	513.8	0.055

Table S2. The size distribution of 5-MQB in the different solvent systems. Concentration = 10^{-5} M.

	particle size (nm)	Polydispersity
$V_{H_2O} : V_{DMA} = 7:3$	156.1	0.055
$V_{H_2O} : V_{DMA} = 8:2$	353.8	0.048
$V_{H_2O} : V_{DMA} = 9:1$	656.7	0.086

Table S3. The size distribution of 5-QPA in the different solvent systems. Concentration = 10^{-5} M.

	particle size (nm)	Polydispersity
$V_{H_2O} : V_{DMA} = 7:3$	353.4	0.018
$V_{H_2O} : V_{DMA} = 8:2$	652.3	0.022
$V_{H_2O} : V_{DMA} = 9:1$	956.6	0.046

Table S4. The size distribution of 5-MPQ in the different solvent systems. Concentration = 10^{-5} M.

	particle size (nm)	Polydispersity
$V_{H_2O} : V_{DMA} = 7:3$	168.7	0.047
$V_{H_2O} : V_{DMA} = 8:2$	353.4	0.066
$V_{H_2O} : V_{DMA} = 9:1$	566.8	0.051

Table S5. The size distribution of 5-MQB with different concentrations Fe^{3+}

Fe^{3+} concentrations (μM)	particle size (nm)	Polydispersity
1.0	138.4	0.088
5.0	145.1	0.077
10.0	196.3	0.075
50.0	286.7	0.087
100.0	335.4	0.092
500.0	413.3	0.120

Spectroscopic Data

UV-vis Absorption Spectra

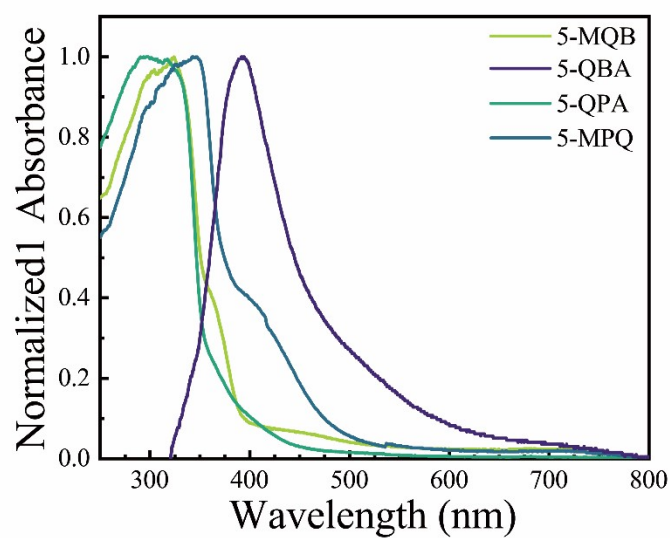


Figure S9. The solid-state UV-vis absorption spectra of 5-MQB, 5-QBA, 5-QPA and 5-MPQ.

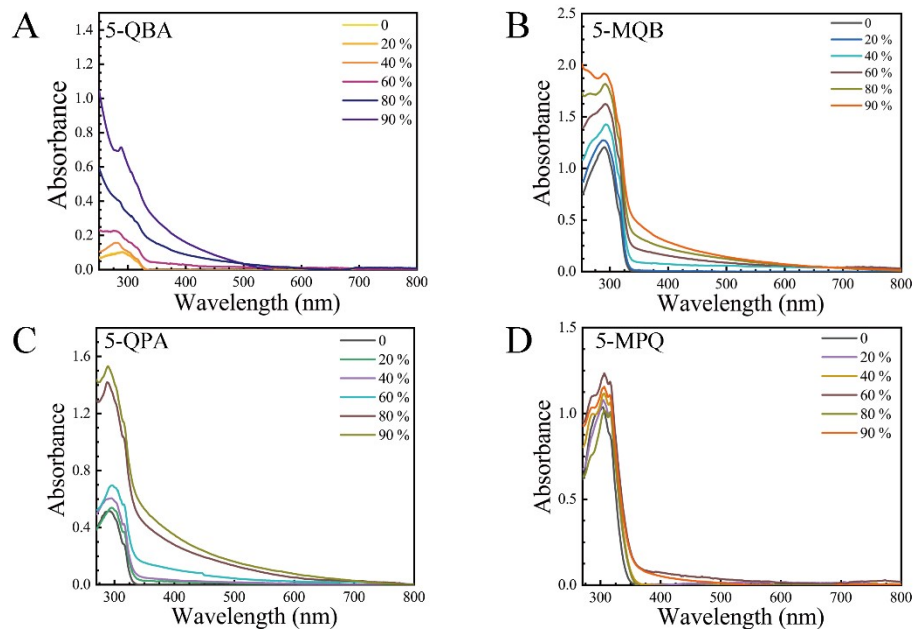


Figure S10. A-D The UV-vis absorption spectra of 5-MQB, 5-QBA, 5-QPA and 5-MPQ in different water fraction.

Solid State Excitation and Emission Spectra

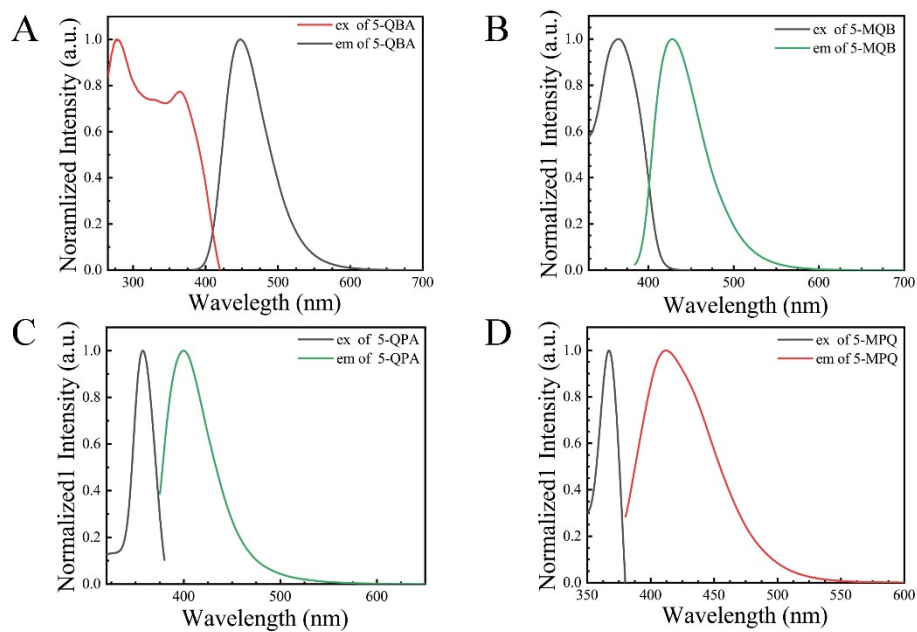


Figure S11. The solid-state excitation and emission wavelength of 5-MQB, 5-QBA, 5-QPA and 5-MPQ.

Fluorescence Lifetime of Solid State.

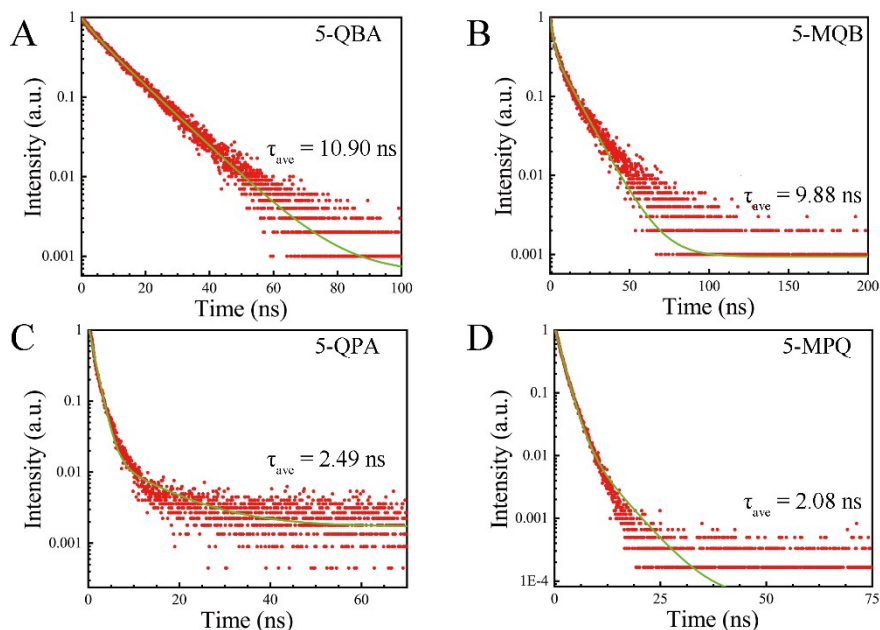


Figure S12. The solid-state fluorescence lifetime of 5-MQB, 5-QBA, 5-QPA and 5-MPQ.

The Fluorescence Spectroscopy of Liquid State.

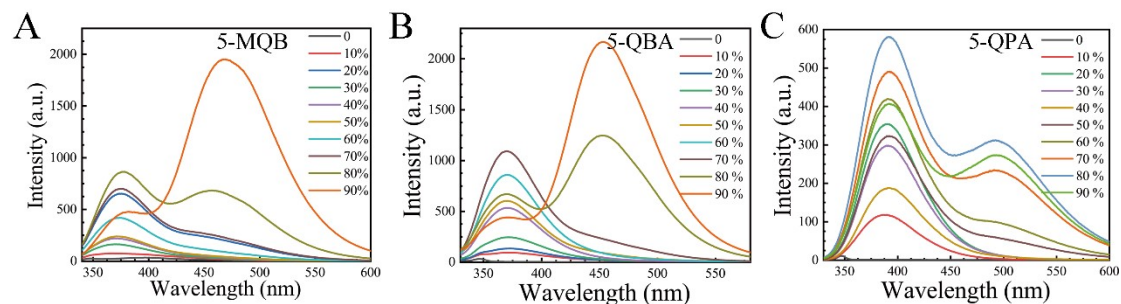


Figure S13. (A) PL spectra of 5-MQB in glycerol/DMA mixtures with different glycerol. $c = 10^{-5}$ M, $\lambda_{\text{ex}} = 316$ nm. (B) PL spectra of 5-QBA in glycerol/DMA mixtures with different glycerol. $c = 10^{-5}$ M, $\lambda_{\text{ex}} = 315$ nm. (C) PL spectra of 5-QPA in glycerol/DMA mixtures with different glycerol. $c = 10^{-5}$ M, $\lambda_{\text{ex}} = 315$ nm.

Fluorescence Lifetime and Quantum Yield of Liquid State.

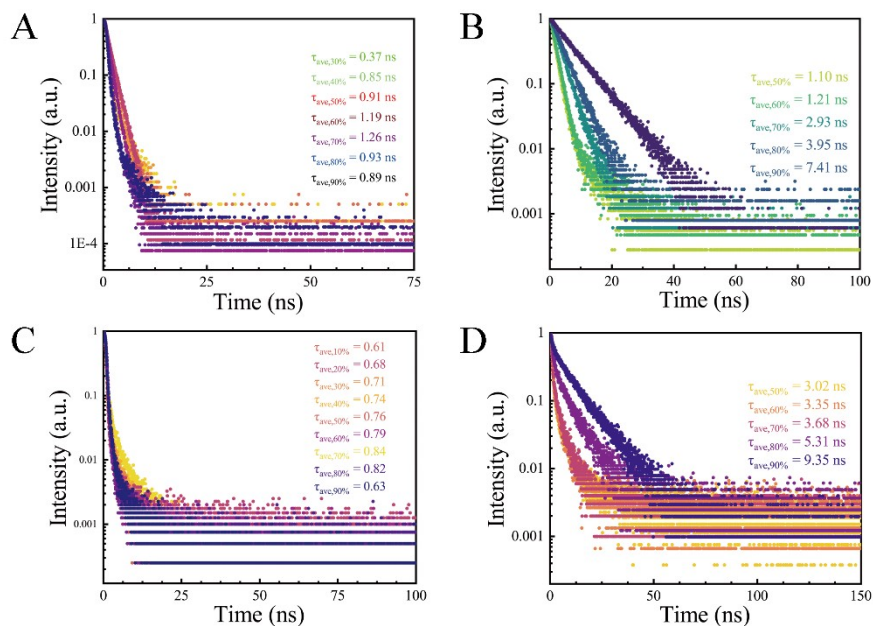


Figure S14. (A) The lifetime of 5-QBA at 375 nm in different water fraction. (B) The lifetime of 5-QBA at 470 nm in different water fraction. (C) The lifetime of 5-QBA at 375 nm in different glycerol fraction. (D) The lifetime of 5-QBA at 470 nm in different glycerol fraction.

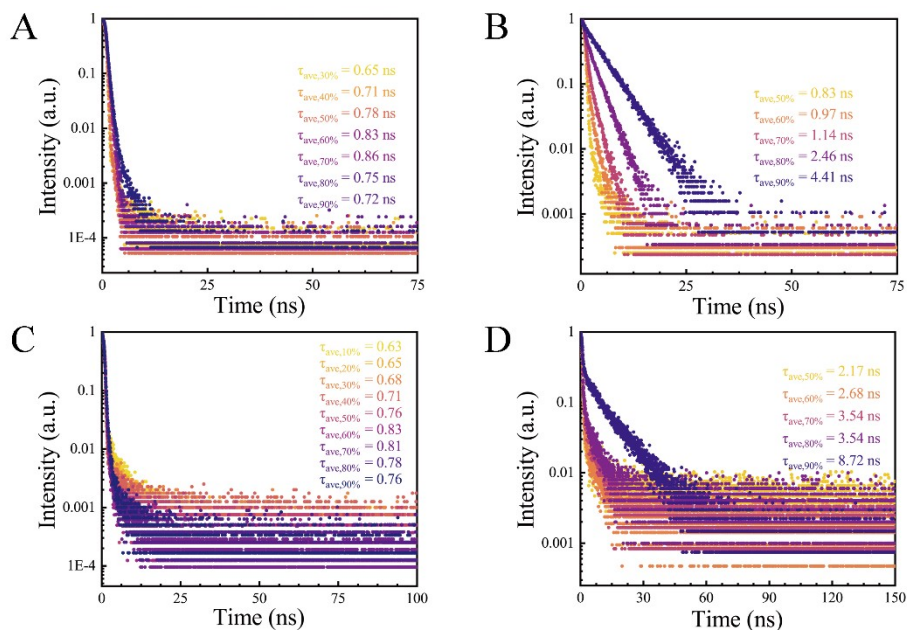


Figure S15. (A) The lifetime of 5-MQB at 365 nm in different water fraction. (B) The lifetime of 5-MQB at 457 nm in different water fraction. (C) The lifetime of 5-MQB at 365 nm in different glycerol fraction. (D) The lifetime of 5-MQB at 457 nm in different glycerol fraction.

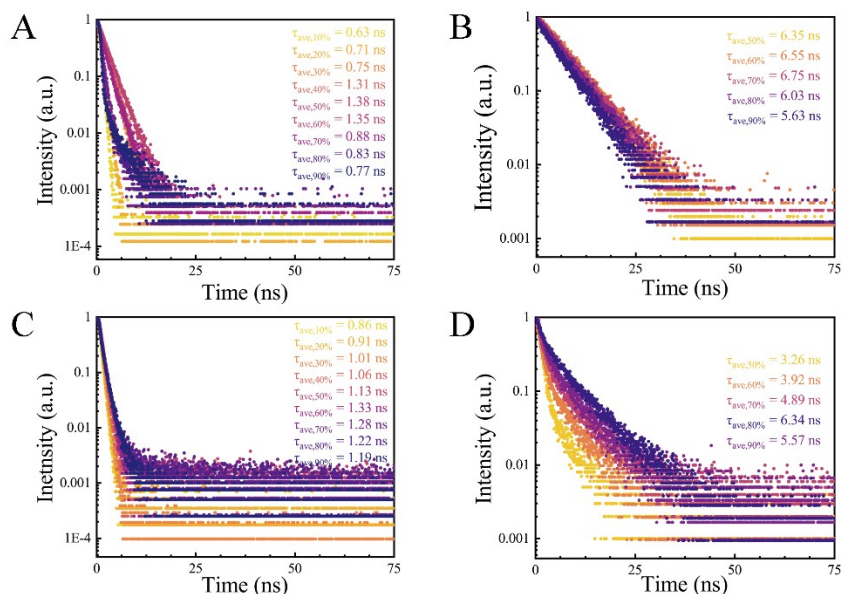


Figure S16. (A) The lifetime of 5-QPA at 385 nm in different water fraction. (B) The lifetime of 5-QPA at 500 nm in different water fraction. (C) The lifetime of 5-QBA at 385 nm in different glycerol fraction. (D) The lifetime of 5-QPA at 500 nm in different glycerol fraction.

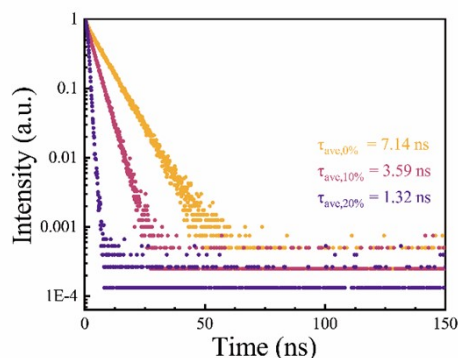


Figure S17. The lifetime of 5-MPQ at 410 nm in different water fraction

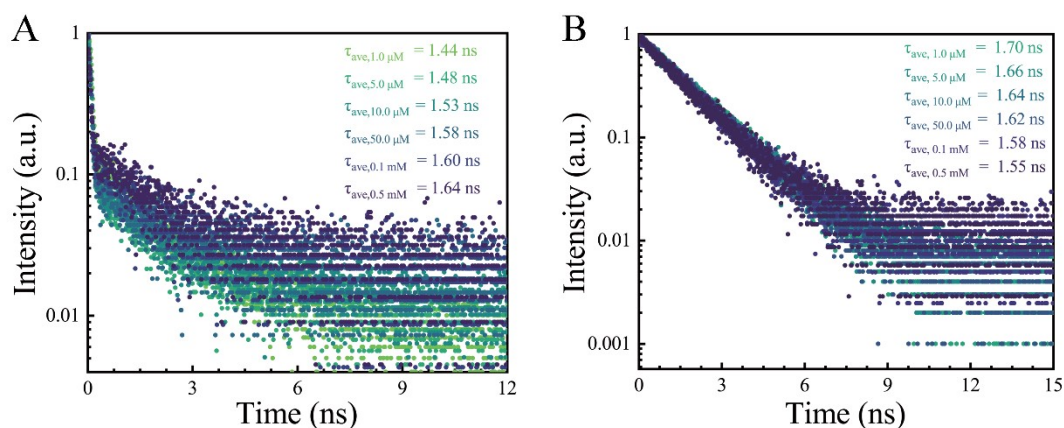


Figure S18. (A) The lifetime of 5-MQB at 375 nm with different concentrations of Fe^{3+} . (B) The lifetime of 5-MQB at 457 nm with different concentrations of Fe^{3+} .

Table S6. The photophysical parameters of 5- QBA in different water fraction. Φ_f = fluorescence quantum yield, k_r = radiative decay rate constant = Φ_f / τ_f , k_{nr} = nonradiative decay rate constant = $(1 - \Phi_f) / \tau_f$, where τ_f = fluorescence lifetime.

	τ_f (ns)		Φ_f (%)		k_r ($\times 10^6$ s $^{-1}$)		k_{nr} ($\times 10^6$ s $^{-1}$)	
	375 nm	470 nm	375 nm	470 nm	375 nm	470 nm	375 nm	470 nm
V _{H₂O} : V _{DMA} = 3:7	0.37	-	0.9	-	24.3	-	2678.4	-
V _{H₂O} : V _{DMA} = 4:6	0.85	-	1.4	-	16.5	-	1160	-
V _{H₂O} : V _{DMA} = 5:5	0.91	1.10	1.6	3.2	17.5	29.1	1081.3	880
V _{H₂O} : V _{DMA} = 6:4	1.19	1.21	3.2	4.3	26.9	35.5	813.4	790.9
V _{H₂O} : V _{DMA} = 7:3	1.23	2.93	3.6	5.6	29.3	19.11	783.7	322.18
V _{H₂O} : V _{DMA} = 8:2	0.93	3.95	4.3	18.8	46.2	47.59	1029	205.6
V _{H₂O} : V _{DMA} = 9:1	0.89	7.41	2.9	68.8	32.5	92.8	1091	42.1

Table S7. The photophysical parameters of 5- QBA in different glycerol fraction.

	τ_f (ns)		Φ_f (%)		k_r ($\times 10^6$ s $^{-1}$)		k_{nr} ($\times 10^6$ s $^{-1}$)	
	365 nm	470 nm	365 nm	470 nm	365 nm	470 nm	365 nm	470 nm
V _{gly} : V _{DMA} = 1:9	0.61	-	1.1	-	18.0	-	1621.3	-
V _{gly} : V _{DMA} = 2:8	0.68	-	1.6	-	23.5	-	1447.1	-
V _{gly} : V _{DMA} = 3:7	0.71	-	2.3	-	32.4	-	1376.1	-
V _{gly} : V _{DMA} = 4:6	0.74	-	4.2	-	56.7	-	1294.6	-
V _{gly} : V _{DMA} = 5:5	0.76	3.02	4.9	0.9	64.5	2.9	1251.3	328.2
V _{gly} : V _{DMA} = 6:4	0.79	3.35	5.1	1.1	64.5	3.3	1201.3	295.2
V _{gly} : V _{DMA} = 7:3	0.84	3.68	7.9	7.7	94.0	20.9	1096.4	250.9
V _{gly} : V _{DMA} = 8:2	0.82	5.31	9.2	27.4	112.2	51.6	1107.3	136.7
V _{gly} : V _{DMA} = 9:1	0.63	9.35	6.3	70.3	100.0	75.1	1487.3	31.7

Table S8. The photophysical parameters of 5- MQB in different water fraction.

	τ_f (ns)		Φ_f (%)		k_r ($\times 10^6$ s $^{-1}$)		k_{nr} ($\times 10^6$ s $^{-1}$)	
	365 nm	457 nm	365 nm	457 nm	365 nm	457 nm	365 nm	457 nm
V _{H₂O} : V _{DMA} = 3:7	0.65	-	1.3	-	20.0	-	1518.5	-
V _{H₂O} : V _{DMA} = 4:6	0.71	-	2.8	-	39.4	-	1369.0	-
V _{H₂O} : V _{DMA} = 5:5	0.78	0.83	3.2	3.5	41.0	42.1	1241.0	1162.7
V _{H₂O} : V _{DMA} = 6:4	0.83	0.97	5.5	6.8	66.2	70.1	1138.6	960.8
V _{H₂O} : V _{DMA} = 7:3	0.86	1.14	6.4	9.8	74.4	85.9	1088.4	791.2
V _{H₂O} : V _{DMA} = 8:2	0.75	2.46	8.1	43.2	108.0	175.6	1125.3	230.8
V _{H₂O} : V _{DMA} = 9:1	0.72	4.41	4.2	53.0	58.3	132.2	1330.6	94.6

Table S9. The photophysical parameters of 5- MQB in different glycerol fraction.

	τ_f (ns)		Φ_f (%)		k_r ($\times 10^6$ s $^{-1}$)		k_{nr} ($\times 10^6$ s $^{-1}$)	
	365 nm	457 nm	365 nm	457 nm	365 nm	457 nm	365 nm	457 nm
V _{gly} : V _{DMA} = 1:9	0.63	-	0.5	-	7.9	-	1579.4	-
V _{gly} : V _{DMA} = 2:8	0.65	-	0.6	-	9.23	-	1529.2	-
V _{gly} : V _{DMA} = 3:7	0.68	-	0.9	-	13.23	-	1457.4	-
V _{gly} : V _{DMA} = 4:6	0.71	-	1.2	-	16.9	-	1391.5	-
V _{gly} : V _{DMA} = 5:5	0.76	2.17	3.5	2.3	46.1	10.6	1269.7	450.2
V _{gly} : V _{DMA} = 6:4	0.83	2.68	4.4	5.5	53.1	20.5	1151.8	352.6
V _{gly} : V _{DMA} = 7:3	0.81	3.54	4.8	6.2	59.3	17.5	1175.3	264.9
V _{gly} : V _{DMA} = 8:2	0.78	3.54	5.6	15.4	71.8	15.8	1210.3	266.7
V _{gly} : V _{DMA} = 9:1	0.76	8.72	3.9	60.3	114.7	69.2	1201.1	45.5

Table S10. The photophysical parameters of 5- QPA in different water fraction.

	τ_f (ns)		Φ_f (%)		k_r ($\times 10^6$ s $^{-1}$)		k_{nr} ($\times 10^6$ s $^{-1}$)	
	385 nm	500 nm	385 nm	500 nm	385 nm	500 nm	385 nm	500 nm
V _{H₂O} : V _{DMA} = 1:9	0.63	-	1.3	-	20.6	-	1566.7	-
V _{H₂O} : V _{DMA} = 2:8	0.71	-	1.9	-	26.7	-	1381.7	-
V _{H₂O} : V _{DMA} = 3:7	0.75	-	2.1	-	28	-	1305.3	-
V _{H₂O} : V _{DMA} = 4:6	1.31	-	2.7	-	20.6	-	742.7	-
V _{H₂O} : V _{DMA} = 5:5	1.38	6.35	3.2	0.9	23.2	1.4	701.4	156.1
V _{H₂O} : V _{DMA} = 6:4	1.35	6.55	4.5	1.5	33.3	2.3	707.4	150.4
V _{H₂O} : V _{DMA} = 7:3	0.88	6.75	3.9	2.5	44.3	3.7	1092.1	144.4
V _{H₂O} : V _{DMA} = 8:2	0.83	6.03	2.5	2.7	30.1	4.5	1174.7	161.4
V _{H₂O} : V _{DMA} = 9:1	0.77	5.36	0.9	2.1	11.7	3.9	1287.1	182.6

Table S11. The photophysical parameters of 5- QPA in different glycerol fraction.

	τ_f (ns)		Φ_f (%)		k_r ($\times 10^6$ s $^{-1}$)		k_{nr} ($\times 10^6$ s $^{-1}$)	
	385 nm	500 nm	385 nm	500 nm	385 nm	500 nm	385 nm	500 nm
V _{gly} : V _{DMA} = 1:9	0.86	-	2.5	-	29.1	-	1133.7	-
V _{gly} : V _{DMA} = 2:8	0.91	-	3.2	-	35.2	-	1063.7	-
V _{gly} : V _{DMA} = 3:7	1.01	-	3.7	-	36.6	-	953.5	-
V _{gly} : V _{DMA} = 4:6	1.06	-	4.2	-	39.7	-	903.8	-
V _{gly} : V _{DMA} = 5:5	1.13	3.26	4.5	2.1	39.8	6.4	845.1	300.3
V _{gly} : V _{DMA} = 6:4	1.33	3.92	5.2	2.9	39.1	7.4	712.8	247.7
V _{gly} : V _{DMA} = 7:3	1.28	4.89	5.9	3.7	46.1	7.6	735.9	196.9
V _{gly} : V _{DMA} = 8:2	1.22	6.34	6.8	4.1	55.7	6.5	763.9	151.3
V _{gly} : V _{DMA} = 9:1	1.19	5.57	5.5	3.4	46.2	6.1	794.1	173.4

Table S12. The photophysical parameters of 5-MPQ in different glycerol fraction.

	τ_f (ns)	Φ_f (%)	$k_r (\times 10^6 \text{ s}^{-1})$	$k_{nr} (\times 10^6 \text{ s}^{-1})$
$V_{\text{H}_2\text{O}} : V_{\text{DMA}} = 0$	7.14	10.3	14.2	125.6
$V_{\text{H}_2\text{O}} : V_{\text{DMA}} = 1:9$	3.59	17.6	49.1	229.5
$V_{\text{H}_2\text{O}} : V_{\text{DMA}} = 2:8$	1.32	6.7	50.8	706.8

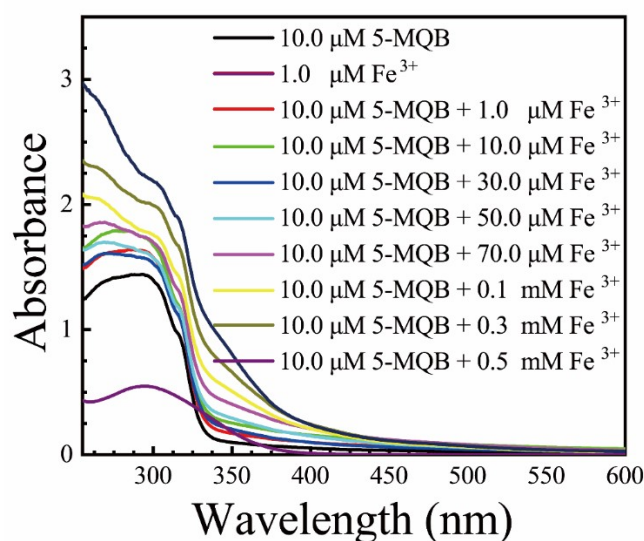
Table S13. Detection of Fe^{3+} in Green Lake Water Samples

added (μM)	found (μM)	recovery (%)	RSD (% , n = 3)
0	3.42	0	1.6
5	8.335	98.30	2.1
15	18.517	100.64	2.7
30	33.159	99.13	3.2

Table S14. The photophysical parameters of 5- MQB with different concentrations of Fe^{3+} .

Fe^{3+} concentrations (μM)	τ_f (ns)		Φ_f (%)		$k_r (\times 10^6 \text{ s}^{-1})$		$k_{nr} (\times 10^6 \text{ s}^{-1})$	
	365 nm	457 nm	365 nm	457 nm	365 nm	457 nm	365 nm	457 nm
1.0	1.44	1.70	7.3	35.8	50.7	210.6	643.8	377.6
5.0	1.48	1.66	6.6	42.2	44.6	254.2	631.1	348.2
10.0	1.53	1.64	4.2	53.1	27.5	323.8	626.1	285.9
50.0	1.58	1.62	3.1	59.4	19.6	366.7	613.3	250.6
100.0	1.60	1.58	2.4	62.3	15.0	394.3	610.2	238.6
500.0	1.64	1.55	1.9	66.9	11.6	431.6	598.2	213.5

Other Spectroscopic Data

**Figure S19.** The UV-vis absorption spectra of 5-MQB with different concentrations of Fe^{3+} .

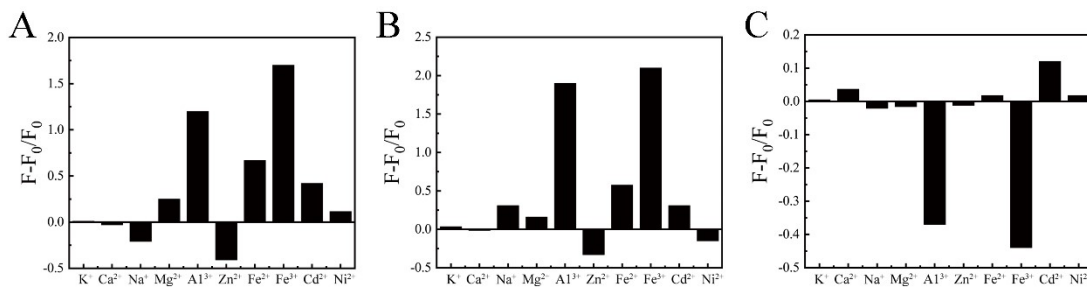


Figure S20. (A) Response selectivity of the 5-QBA to different metal ions, (B) Response selectivity of the 5-QPA to different metal ions, (C) Response selectivity of the 5-MPQ to different metal ions.

XPS Data:

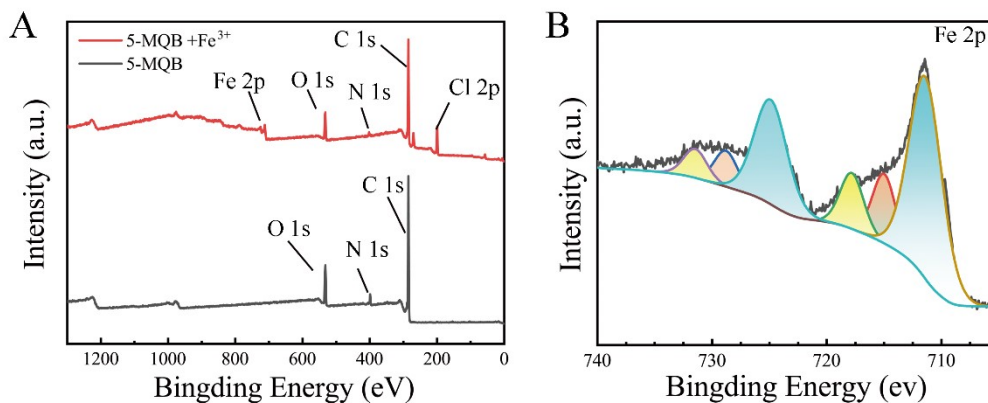


Figure S21. (A) XPS survey spectra of 5-MQB and 5-MQB with Fe^{3+} . (B) Fe 2p core-level XPS spectra of 5-MQB with Fe^{3+} .

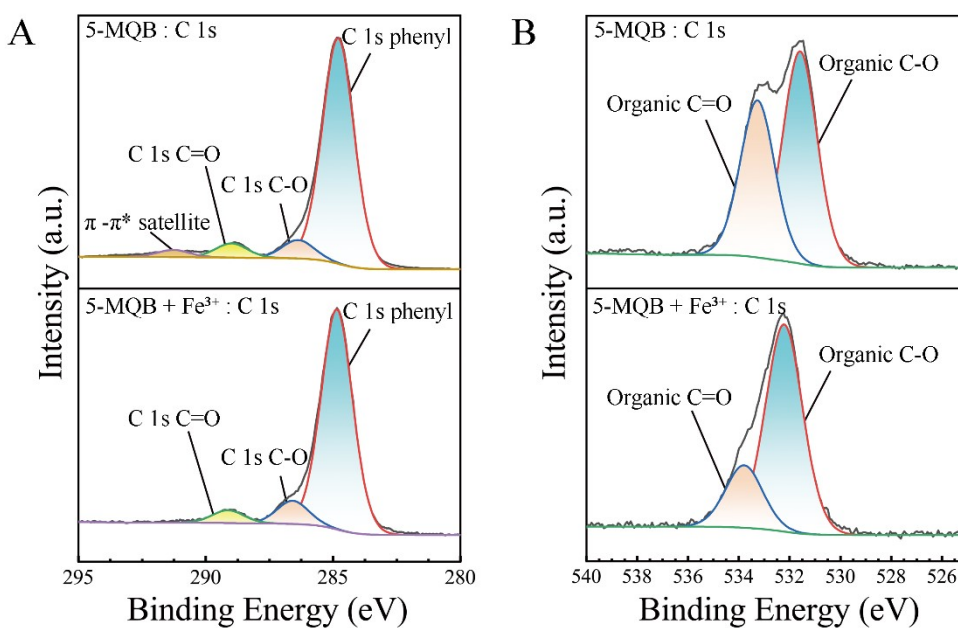


Figure S22. C 1s (A) and N 1s (B) core-level XPS spectra of 5-MQB and 5-MQB with

Fe³⁺.

The Crystal Structure of Compounds.

Table S15. Summary of crystallographic data and structural refinements

Compound	5-MQB	5-QBA	5-QPA	5-MPQ
CCDC number	2255887	2255888	2255889	2255886
Empirical formula	C ₁₇ H ₁₃ NO ₂	C ₁₆ H ₁₁ NO ₂	C ₁₇ H ₁₃ NO ₂	C ₁₆ H ₁₃ NO
Formula weight	263.28	249.26	263.28	235.27
Temperature/K	300.98(10)	296.15	293(2)	235.27
Crystal system	monoclinic	monoclinic	monoclinic	monoclinic
Space group	P2 ₁	P2 ₁ /c	P2 ₁ /n	P2 ₁ /c
<i>a</i> /Å	11.1492(12)	10.278(2)	9.7854(5)	7.6245(11)
<i>b</i> /Å	4.0685(4)	7.3347(16)	10.5351(4)	7.2463(10)
<i>c</i> /Å	14.1566(17)	15.573(5)	13.0707(6)	21.937(3)
α /°	90	90	90	90
β /°	95.372(10)	97.695(11)	107.184(5)	93.996(8)
γ /°	90	90	90	90
Volume/Å ³	639.33(12)	1163.4(5)	1287.31(11)	1209.0(3)
<i>Z</i>	2	4	4	4
Density/ g.cm ⁻³	1.368	1163.4(5)	1.358	1.293
F (000)	276.0	520.0	552.0	496.0
μ /mm ⁻¹	0.090	0.095	0.090	0.409
Goodness-of-fit on F ²	1.145	1.060	1.116	0.981
<i>R</i> _I [<i>I</i> >= 2 σ (<i>I</i>)] ^b	0.0965	0.0685	1.116	0.0447
<i>wR</i> ₂ [<i>I</i> >= 2 σ (<i>I</i>)] ^c	0.2505	0.1752	0.2419	0.1317
<i>R</i> _I [all data] ^b	0.1348	0.0870	0.1233	0.0610
<i>wR</i> ₂ [all data] ^c	0.2698	0.1947	0.2565	0.0610

Calculation

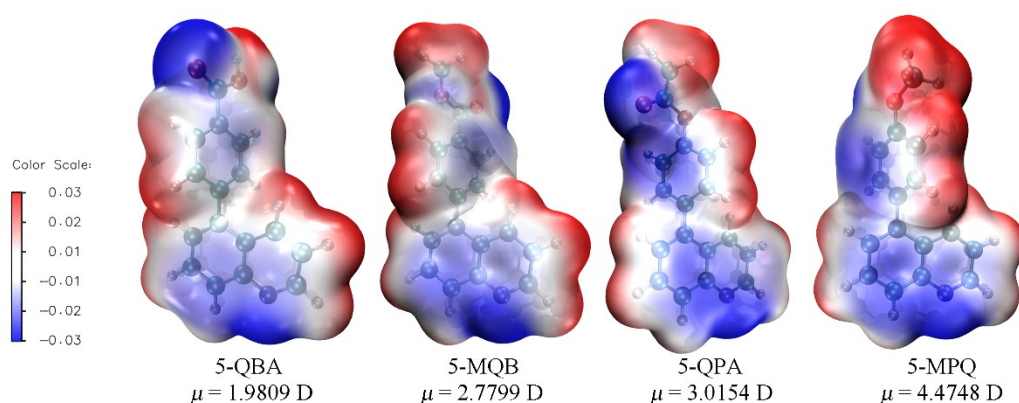
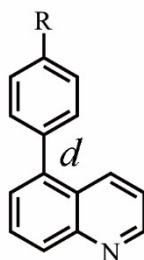


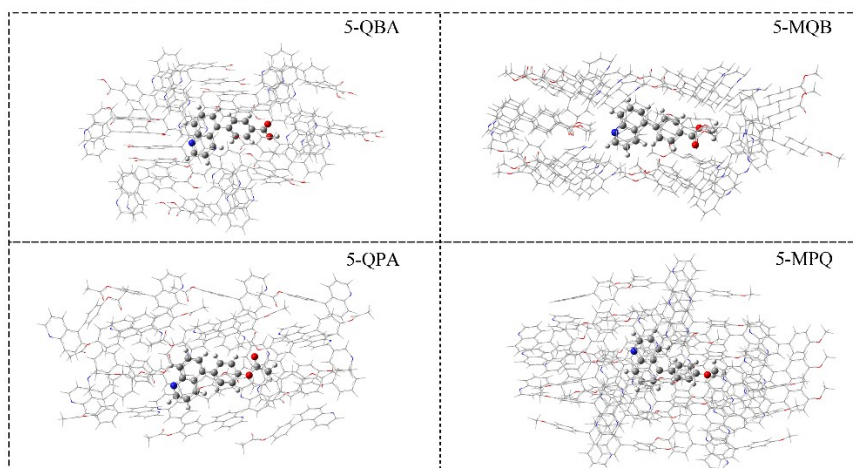
Figure S23. The ESP maps and dipole moment of compounds.

Table S16. Calculated C–C Atomic Distances and dihedral angles of compounds and their derivatives in the ground (S_0) and excited states (S_1) based on isolated phase, calculated by the TD-DFT, PBE0/Def2-SVP level, gaussian 09 program.



compound	State	Atomic Distance (Å) d	Dihedral Angle ($^\circ$) P_1 and P_2
5-MQB	S_0	1.48472	52.40994
	S_1	1.42851	25.22277
5-QBA	S_0	1.48456	52.43515
	S_1	1.42886	25.36345
5-QPA	S_0	1.48526	52.63170
	S_1	1.43619	26.93252
5-MPQ	S_0	1.48413	51.40477
	S_1	1.44340	30.00669

Table S17. Calculated C–C Atomic Distances and dihedral angles of compounds and their derivatives in the ground (S_0) and excited states (S_1) based on isolated phase, calculated by the ONION model, the QM part used PBE0/def2svp level, the MM part used UFF in gaussian 09 program.



compound	State	Atomic Distance (Å) d	Dihedral Angle ($^\circ$) P_1 and P_2	RMSD S_0 Vs S_1
5-QBA	S_0	1.48134	60.33128	0.065
	S_1	1.47570	57.03277	
5-MQB	S_0	1.48429	46.96033	0.2721
	S_1	1.47439	44.05341	
5-QPA	S_0	1.48166	46.04247	0.1953
	S_1	1.44584	39.99062	
5-MPQ	S_0	1.47993	47.04038	0.1260
	S_1	1.44924	38.75792	

References

1. Gaussian 09, Revision E.01 M. J. Frisch, G. W. Trucks, H. B. Schlegel, G. E. Scuseria, M. A. Robb, J. R. Cheeseman, G. Scalmani, V. Barone, B. Mennucci, G. A. Petersson, H. Nakatsuji, M. Caricato, X. Li, H. P. Hratchian, A. F. Izmaylov, J. Bloino, G. Zheng, J. L. Sonnenberg, M. Hada, M. Ehara, K. Toyota, R. Fukuda, J. Hasegawa, M. Ishida, T. Nakajima, Y. Honda, O. Kitao, H. Nakai, T. Vreven, J. A. Montgomery, Jr., J. E. Peralta, F. Ogliaro, M. Bearpark, J. J. Heyd, E. Brothers, K. N. Kudin, V. N. Staroverov, T. Keith, R. Kobayashi, J. Normand, K. Raghavachari, A. Rendell, J. C. Burant, S. S. Iyengar, J. Tomasi, M. Cossi, N. Rega, J. M. Millam, M. Klene, J. E. Knox, J. B. Cross, V. Bakken, C. Adamo, J. Jaramillo, R. Gomperts, R. E. Stratmann, O. Yazyev, A. J. Austin, R. Cammi, C. Pomelli, J. W. Ochterski, R. L. Martin,

K. Morokuma, V. G. Zakrzewski, G. A. Voth, P. Salvador, J. J. Dannenberg, S. Dapprich, A. D. Daniels, O. Farkas, J. B. Foresman, J. V. Ortiz, J. Cioslowski, and D. J. Fox, Gaussian, Inc., Wallingford CT, 2013.

2. J. R. Reimers. *J. Chem. Phys.*, 2001, **115**, 9103-9109.
3. T. Lu and F. Chen. *J Comput. Chem.*, 2012, **33**, 580-592.
4. P. R. Spackman, M. J. Turner, J. J. Mckinnon, S. K. Wolff, D. J. Grimwood, D. Jayatilaka and M. A. Spackman. *J Appl. Crystallogr.*, 2021, **54**, 1006-1011.
5. Dolomanov, O.V.; Bourhis, L.J.; Gildea, R.J.; Howard, J.A.K.; Puschmann, H., OLEX2: A complete structure solution, refinement and analysis program. *J. Appl. Cryst.*, 2009, **42**, 339-341